MICROBIAL ECOLOGY

Microb Ecol (2000) 40:85–93
DOI: 10.1007/s002480000062

Artificial Cyanobacterial Mats: Growth, Structure, and Vertical Zonation Patterns

T. Fenchel, M. Kühl

Marine Biological Laboratory, University of Copenhagen, Strandpromenaden 5, DK-3000 Helsingør, Denmark

Received: 20 December 1999; Accepted: 10 June 2000; Online Publication: 28 August 2000

Abstract

The formation of cyanobacterial mats (originally induced by incubation of sediment cores in which metazoans and most other eukaryotes had been removed) was followed over approximately 2.6 years. The thickness of the mats increased at a rate of 2–3 mm per year because of accumulation of empty cyanobacterial sheaths and as a result of carbonate deposition; the fraction of living biomass remained relatively constant over at least 2 years, but there was a slow accumulation of nonliving organic C (≈ 1 mmol yr^{-1}). Biota composition (dominated by five types of filamentous cyanobacteria, unicellular cyanobacteria, diatoms, anoxygenic phototrophs, and heterotrophic bacteria) and vertical zonation patterns in the upper 2–3 mm of the mats were also almost constant over time. Using transmission electron microscopy and stereological analysis it was possible to quantify the vertical distribution of major groups of organisms.

Introduction

It has previously been shown that cyanobacterial mats develop when sediment cores (collected in a shallow brackish bay) are deprived of metazoans and incubated in the light [9–11]. These mats resembled natural cyanobacterial mats in most respects, and they grew to a thickness of about 2 mm within a year. These mats have now been allowed to grow for altogether approximately 2.6 years and have attained a thickness of about 7 mm. During this period, the mats have developed the characteristic mechanical properties of cyanobacterial mats otherwise known especially from hyperhaline habitats [cf., 2–4, 12, 13].

Correspondence to: T. Fenchel; Fax: +4549261165; E-mail: mbltf@inet.uni2.dk

The purpose of the present study is to present a detailed qualitative and quantitative description of these mats; a subsequent paper [14] describes properties of spectral light absorption, the vertical distribution of photosynthetic pigments, and photosynthetic and respiratory activity.

Materials and Methods

Sediment cores were originally defaunated by freezing (at −20°C for 20 h) and maintained as described in [9]. Briefly, they were kept in aquaria with air bubbled seawater (salinity: ≈ 18 ppt, maintained by occasionally adding distilled water to compensate for evaporation). The mats were exposed to light (about 300 μmol photons $m^{-2}s^{-1}$) from 120 W halogen light bulbs with a 14-h light: 10 h dark cycle; temperature ranged from 17°C in the dark to 25°C after some hours of illumination.

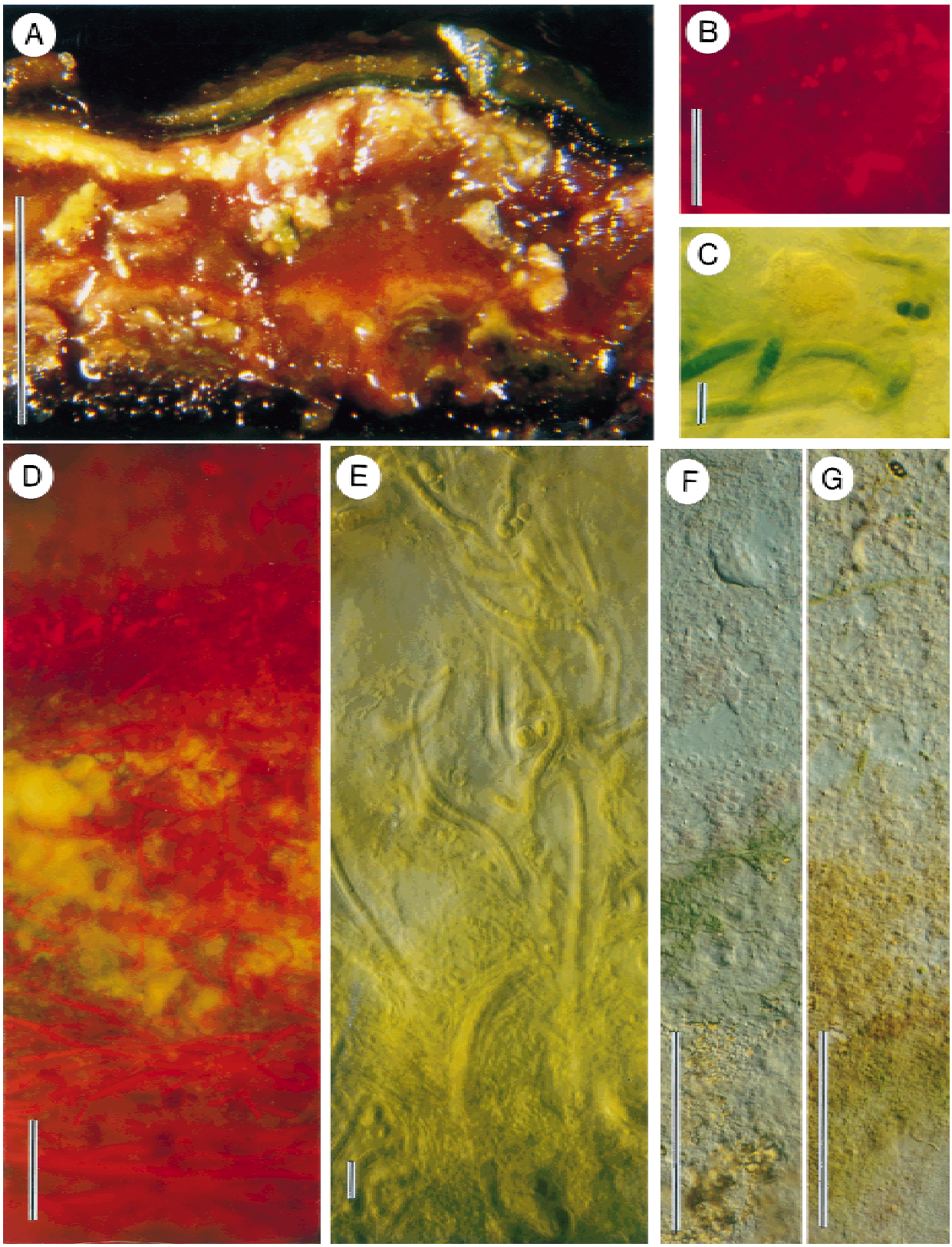

Fig. 1. (A) Macroscopic appearance of a 2.6-year-old mat; scale bar: 5 mm. (B–G) Freeze sections of the mat. (B) Unicellular cyanobacteria at 2.1 mm depth, green light fluorescence; scale bar: 0.1 mm. (C) *Phormidium* filaments and a *Thiocapsa* colony, 0.4 mm depth; scale bar: 10 μm. (D) Upper millimeter of the mat, blue light fluorescence, showing especially the *Calothrix* filaments at the top and *Phormidium* filaments toward the bottom; scale bar: 0.1 mm. (E) Surface mucous layer showing filaments of *Calothrix* and *Pseudanabaena* and bacteria; scale bar: 10 μm. (F) Deep layer of *Pseudanabaena* 3 filaments, the middle of the photograph is at 2 mm depth; scale bar: 0.1 mm. (G) Section showing colors of purple and green phototroph bacteria; the middle of the photograph is at 3.2 mm depth; scale bar: 0.1 mm.

Dry matter and dry organic matter was measured by weighing 1 cm^2 pieces of fresh mat, after drying to constant weight at 110°C, and again after dry combustion at 550°C. Carbonate was measured by placing dried pieces of mat in 1 N HC1 for 24 h in gas-tight vials and measuring the evolved CO_2 in the gas phase. Thickness, carbonate contents, and organic C were determined on different mats originating from June, September, and December 1996, respectively.

Microscopical work was based on a mat originating from December 1996. Sections for light microscopy were prepared by cutting pieces of the mat with a razor blade (about 7 mm deep and with a cross section of about 5 × 5 mm) and immersing them in liquid N_2 for a few seconds. The frozen mat pieces were kept at −20°C and eventually sectioned (20–30 μm) with a cryotome. Sections were imbedded in Gurr's water mounting medium (which—in contrast to glycerol–gelatin—proved not to be autofluorescent). They were viewed and photographed with different modes of transmitted light microscopy and with epifluorescence microscopy using either blue or green excitation light. Slides kept at 5°C in the dark retained their fluorescence and pigment absorption (chlorophyll *a*, bacteriochlorophylls, carotenoids, and phycobilines) for at least 6 months [14].

For transmission electron microscopy, a piece of mat was sectioned horizontally with a razor blade into approximately 1-mm-thick slices. Each of these were immediately fixed in 3% glutaraldehyde in phosphate buffer (pH 7.5), rinsed in buffer, postfixed in 1% OsO_4, rinsed in water, stained with uranyl acetate, dehydrated in an ethanol series, and embedded in epon. Sections (0.1 μm) were cut on a LKB-microtome and viewed with a Zeiss EM900 electron microscope. For quantification of the biota, an almost complete series of sections, covering the mat to a depth of 5.4 mm, was photographed at a magnification of 1000× (altogether 100–200) μm of mat were lost mainly because carbonate deposits caused difficulties in sectioning at some horizons). Additional photographs were made at all depths at higher magnifications.

Estimates of quantitative properties of the mats were based on TEM-photographs and the application of stereological methods [1, 7]. The biovolume of different mat constituents was estimated from volume fraction, V_v, which is identical to area fraction, V_a [1]. Estimates of area fraction were based on a point grid printed on a transparent overlay and by counting points that covered sections of interest. Total lengths of cyanobacterial filaments could be calculated for each species from volume fraction and cross-sectional area of the filaments. Numbers of bacteria per unit volume of mat were calculated from the number of sections of bacteria per unit area of sectioned mats, N_a, and volume fraction as $N_v = [K(N_a)^{3/2}]/[\beta(V_v)^{1/2}]$, where K (ranging between 1.02 and 1.1) is a factor correcting for size variation of the particles and β is a shape coefficient. Assuming cylindrical shape of bacteria, β could realistically vary between 1.6 and 2.2 [1]. In the present study K and β were chosen as 1.1 and 1.8, respectively. Estimates of volume fraction based on two-dimensional sections are robust and reliable (the main sources of error being possible distortion of the mat during fixation and "lost caps," that is, small, peripheral sections of, e.g., bacterial cells that may be overlooked or incorrectly interpreted).

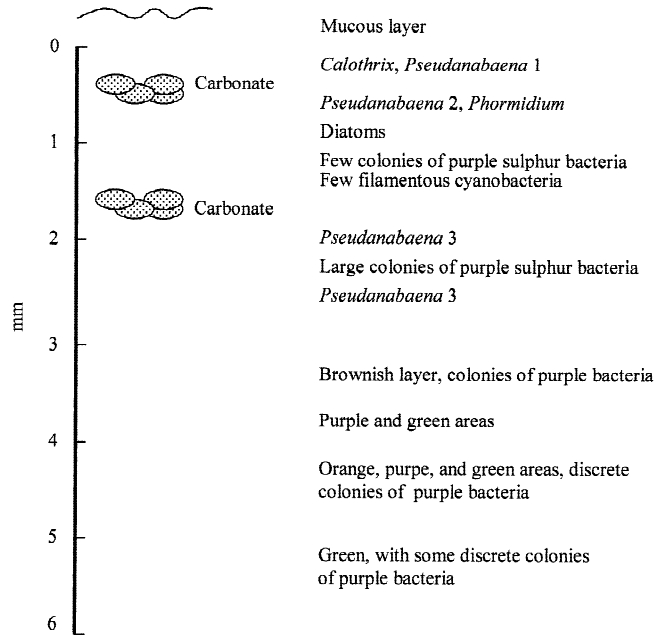

Fig. 2. A schematic presentation of the vertical zonation of the mat.

Estimates of cell numbers, however, are uncertain and not amenable to statistical analysis, because actual size distribution and variation in shape were unknown. Estimates are correct within an order of magnitude and the relative differences in cell densities are reliable when comparing different depths. Large colonies of anoxygenic phototrophic bacteria were estimated separately and cell density was estimated individually for each sectioned colony.

Results

The Biota and Vertical Zonation

The overall structure of the mat, as based on macroscopic observation (Fig. 1A) and freeze sectioned mats (Fig. 1B–G), is summarized in Fig. 2. The uppermost mucous layer was yellowish-brown and varied in thickness between 0.2 and 0.5 mm; its upward extension was not well defined and so the depth scale applied here starts at the base of the mucous surface layer. The layer contained the distal parts of filaments of *Calothrix* and relatively few filaments of a morphotype of *Pseudanabaena* (*Pseudanabaena* 1) in addition to bacteria (Fig. 3A). Underlying this layer was an about 0.3 mm thick layer of densely packed cyanobacterial filaments. The upper part of the zone (Figs. 1E, 3A) consisted of a mixture of *Calothrix* and *Pseudanabaena* 1 filaments. Further down (from 0.3 to 0.4 mm depth) only *Pseudanabaena* 1 occurred; the filaments were oriented parallel to the surface

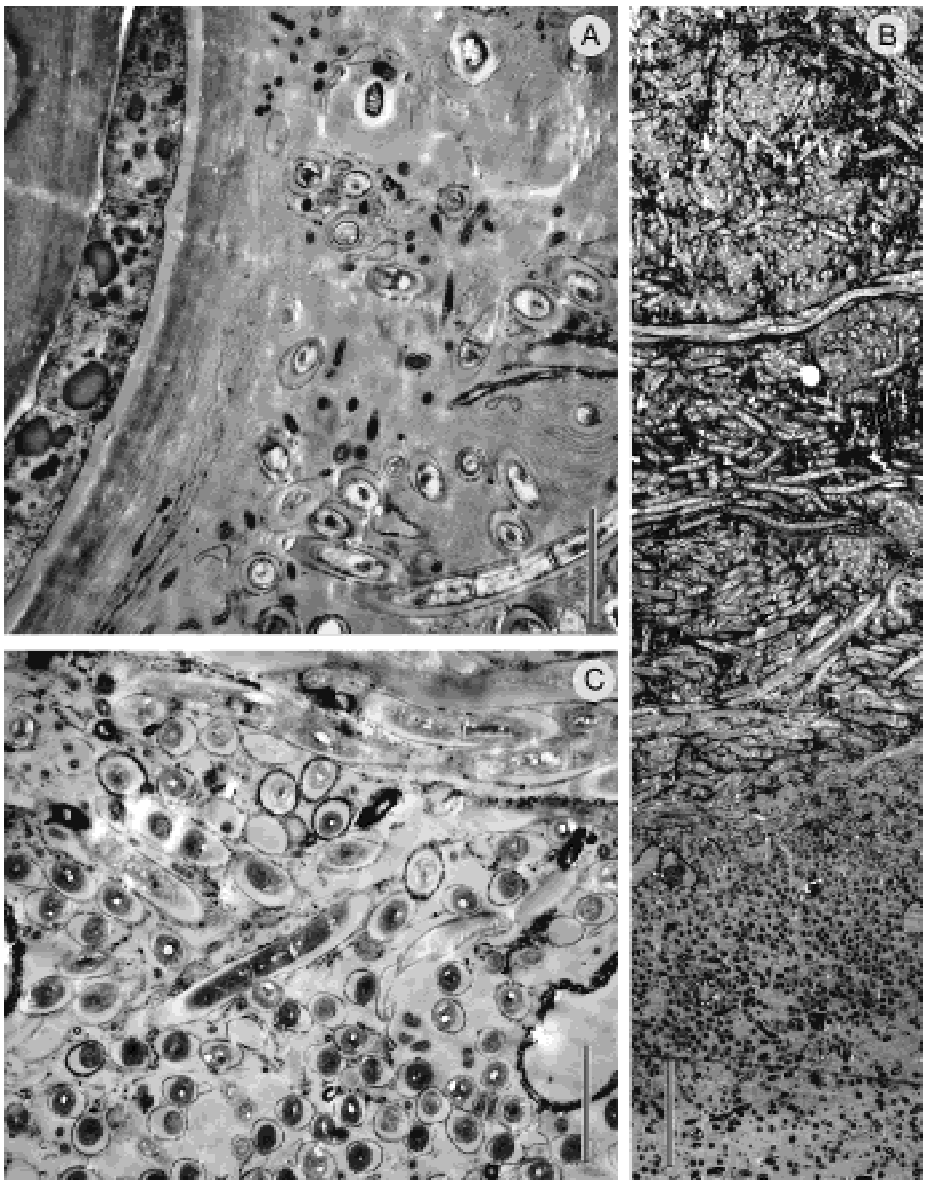

Fig. 3. (A) Mucous surface layer with one *Calothrix* and several *Pseudanabaena* filaments and bacteria: scale bar: 5 μm. (B) Middle of photograph is at 0.44 mm depth; the transition between *Pseudanabaena* 1 and *Pseudanabaena* 2 is seen about 1/3 of the way from below; scale bar: 20 μm. (C) Between 0.31 and 0.53 mm depth, showing two layers of perpendicularly oriented *Pseudoanabaena* filaments; scale bar: 5 μm.

and, within 20–40 μm thick layers, also parallel to each other. The filaments of neighboring layers, however, tended to be oriented more or less perpendicular to one another so that the zone had a plywood structure (Fig. 3B,C). The upper part of the zone was light green, but appeared dark green or almost black at about 0.5 mm depth. Below this depth, *Pseudanabaena* 1 was replaced by another morphotype *Pseudanabaena* 2 (Fig. 3B); the delimitation between these zones was very sharp. The zone beneath 0.5 mm principally continued down to about 1 mm. It also harbored filaments of *Phormidium* (typically oriented parallel to the surface and to one another, see Figs 1D, 4A,B) and diatoms (Fig. 5A); these constituents, however, showed a patchy horizontal distribution in the mat. In some places they were numerous and in other places they were almost absent. This zone also harbored many unicellular cyanobacteria (Fig. 1B) as well as a variety of other types of bacteria; the uppermost colonies of phototrophic purple bacteria (possibly *Thiocapsa*) appeared at a depth of 0.4–0.5 mm (Fig. 1C). This zone (between 0.3 and 1 mm) was in most places interrupted by a 0.2–0.4 mm thick, compact layer of carbonate minerals (seen as a yellowish–whitish layer in Fig. 1A and as yellowish green particles in Fig. 1D) that rendered the mat hard and likely to break or split at this zone when cut. Similar, less developed, discrete carbonate layers occurred in many places at a depth of 1.5–2 mm and sometimes again in the purple zone several mm beneath the surface. Polarization microscopy (Fig. 4C) revealed carbonate formation in the form of small crystals

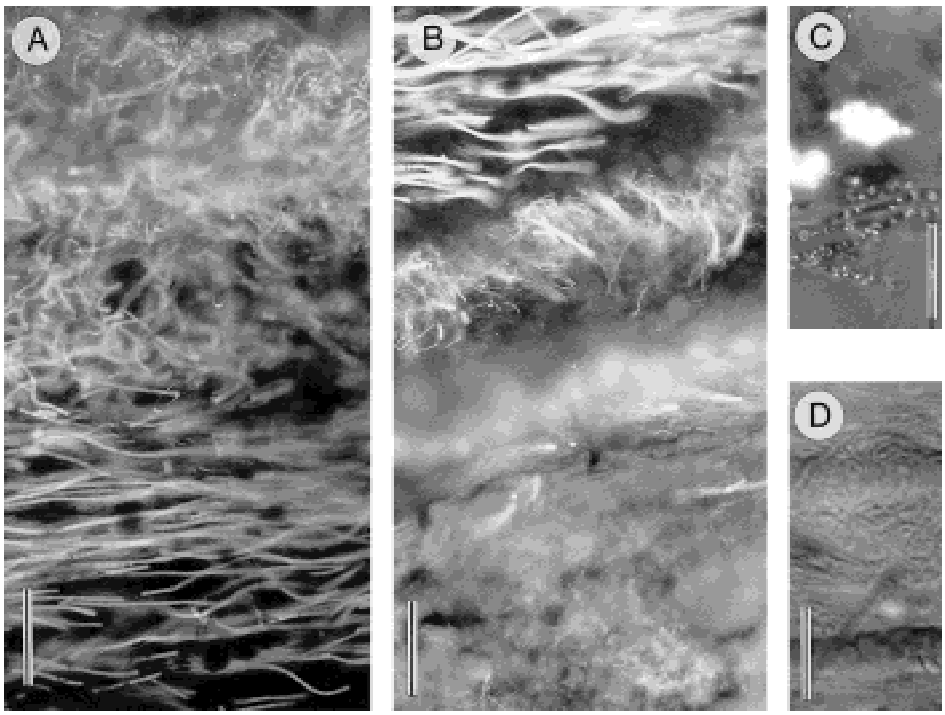

Fig. 4. (A, B) Green fluorescence microscopy of the surface and at 0.3–0.6 mm depth, respectively; scale bars: 50 μm. (C) Polarization microscopy, showing carbonate crystals associated with *Phormidium* sheaths at a depth of about 1 mm; scale bar: 0.1 mm. (D) Bacterial colony associated with a *Phormidium* filament at a depth of about 1 mm; scale bar: 10 μm.

associated with the mucus sheaths of cyanobacteria. Somehow the crystals must eventually become cemented together over time to form several hundred micrometer thick concretions and eventually an almost continuous carbonate layer.

Filamentous cyanobacteria and diatoms were almost absent between 1 and 2 mm depth. A discrete band of what appeared to be *Thiocapsa* colonies appeared at around 2 mm depth (Fig. 5C,D). Between 2 and 3 mm, a green band represented a layer of a third *Pseudanabaena* morphotype (Figs. 1F, 5F). Beneath this layer, sections showed vivid coloration of shades of brown, green, orange and pink (Fig. 1A,G) revealing the presence of various types of anoxygenic phototrophic bacteria. The black, permanent sulfidic zone extended down into the underlying sediment and could therefore not be sectioned.

A variety of unicellular, filamentous, and colony-forming bacteria occurred throughout the mat. Some of these were intimately associated with cyanobacterial filaments (Fig. 4D) or they appeared to be distributed randomly (Fig. 3A,C). Many bacteria showed characteristic morphological traits; this especially applied to phototrophic bacteria, such as the colony-forming purple bacteria with vesicular photosynthetic membranes found in the upper half of the mat (Fig. 5C) and deeper in the mat, a type with stacked membranes that resembles, e.g., *Ectothiorhodospira* (Fig. 6A) and green sulfur bacteria (Fig. 6B). Other bacteria, although showing characteristic traits, could not be identified (Fig. 6C–E).

The uppermost 0.5–1 mm part of the mat was basically made up of filamentous cyanobacteria and their mucous sheaths. A part of mat is made up of carbonate minerals. The largest part, however, is made up of empty cyanobacterial sheaths (Fig. 5B,C) that form the bulk of the gelatinous matrix. Their accumulation is the major cause for the slow, but constant increase in mat thickness. Identifiable cyanobacterial sheaths were evident down to the base of the mat; thus, the empty sheaths must have retained their mechanical integrity for more than 2 years.

The Quantitative Composition of the Biota

Volume fractions of the most important groups of oxygenic phototrophs and of all oxygenic phototrophs together are shown in Fig. 7. As expected, the bulk of the biomass occurred in the upper millimeter of the mat; the minimum evident at 0.7–0.9 mm depth reflects the carbonate layer that takes up most of the available volume. Why oxygenic phototrophs are largely absent between 1 and 2 mm, but reappear between 2 and 3 mm, represented almost exclusively by *Pseudanabaena* 3, is unclear. The integrated biomass (wet weight) of oxygenic phototrophs (assuming a specific density of unity) amounts to about 0.032 g cm^{-2}. The total length of cyanobacterial filaments beneath 1 cm^2 is about 11 km and they represent a surface area of about 345 cm^2.

Volume fractions of all bacteria and of colonial phototrophic bacteria are shown in Fig. 8. Expectedly, bacteria as

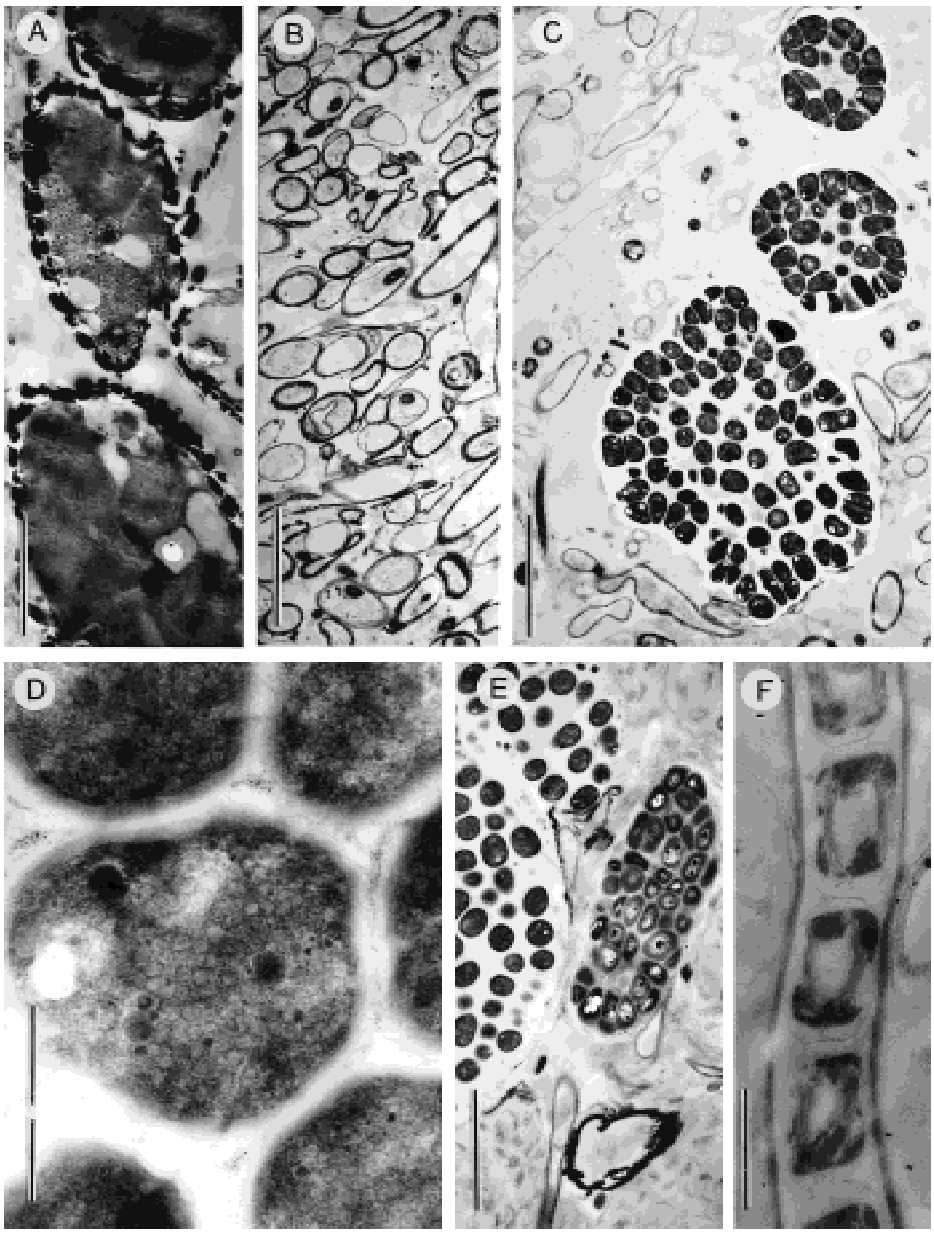

Fig. 5. (A) Diatoms at 0.90 mm depth. (B) Empty *Pseudanabaena* sheaths at a depth of 1.75 mm. (C) Colonies of phototrophic bacteria (possibly *Thiocapsa*) at a depth of 1.85 mm. Scale bars, A–C: 5 μm. (D) As C; scale bar: 0.5 μm. (E) Colonies of phototrophic bacteria at a depth of 2.75 mm; scale bar: 5 μm. (F) Filament of *Pseudanabaena* 3 at a depth of 2.30 mm; scale bar: 1 μm.

a whole are more evenly distributed with depth, but their density is highest immediately beneath the dense layer of oxygenic phototrophs close to the surface of the mat. The mean volume fraction of all bacteria down to 0.6 mm depth was 3.9%, corresponding to a biomass of about 0.023 g cm^{-2} (ww) or somewhat less than that represented by oxygenic phototrophs. The distribution of colonies of anoxygenic phototrophs supports the visual impression that these are distributed in discrete vertical bands. It is also seen that phototrophic bacteria are quantitatively dominating in some horizons (even when noncolonial phototrophs are not included). Bacterial numbers averaged about 6×10^{10} cells ml^{-1}. The density peaks at the depths of 1 and 2.2–2.5 mm, respectively, were almost exclusively due to colony-forming purple bacteria.

Development of the Mats over Time

Figure 9 shows the development of mat thickness, and accumulations of carbonate and organic carbon during about 900 days; data prior to 400 days derive from [11]. The graphs suggest a linear increment with time in all cases and support previous estimates [11] of a net carbonate accumulation of about 0.33 μmol cm^{-2} day^{-1} and a net accumulation of about 2.5 μmol organic C cm^{-2} day^{-1}.

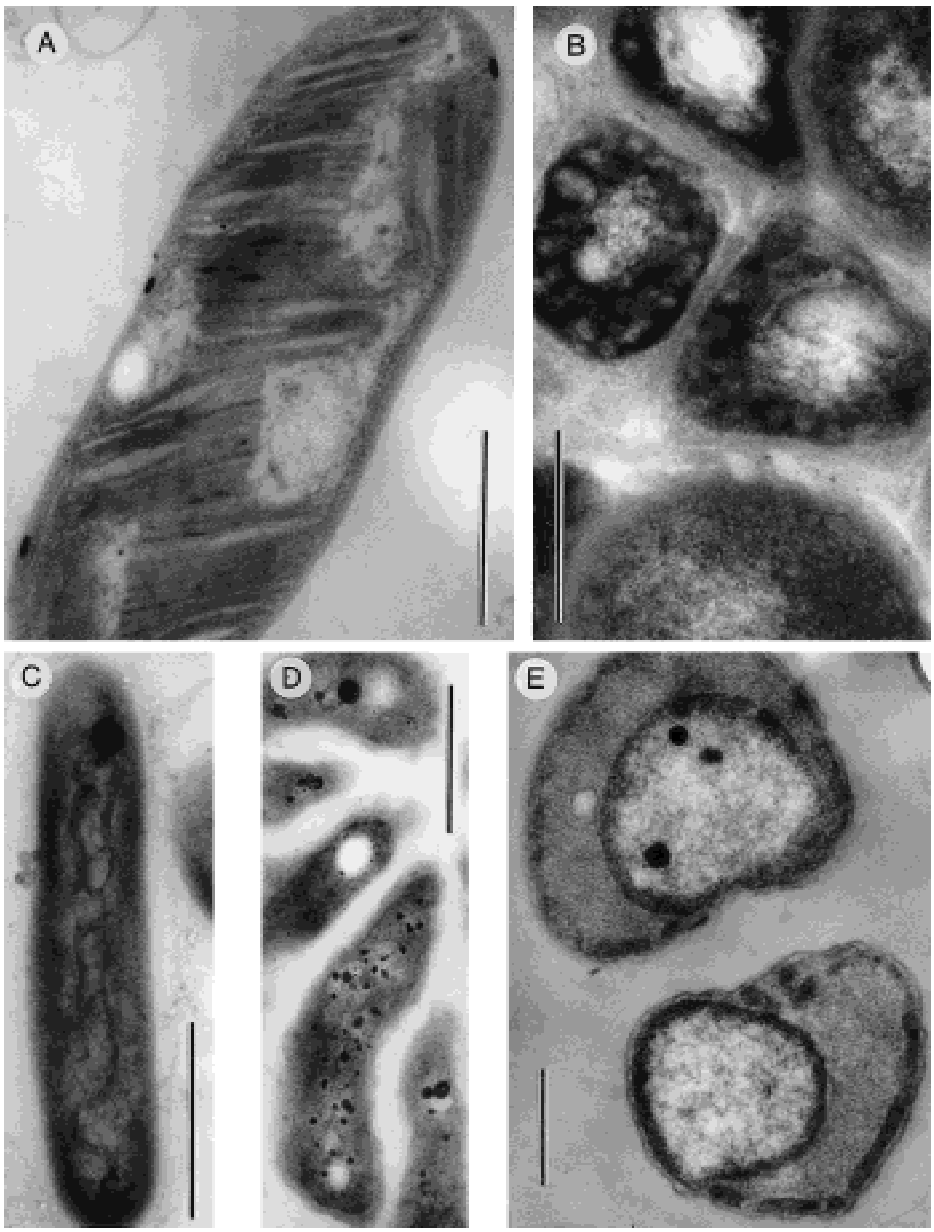

Fig. 6. (A) Phototrophic purple bacterium, depth: 2.60 mm. (B) Green sulfur bacterium, depth: 2.60 mm; scale bars A, B: 0.5 µm. (C–E) Different types of bacteria, C and D from 3.10 mm depth and E from 2.60 mm depth; scale bars: C and E: 0.5 µm, D: 1 µm.

Discussion

Sectioning of microbial mats for light and transmission electron microscopy is often difficult or impossible due to the presence of mineral grains. Previous use of TEM on gelatinous mats [5, 15, 16, 17, 18] has documented its value for the qualitative visualization of zonation patterns and for the identification of, mainly phototrophic, microorganisms and their mutual organization within the mats. The surface layers of the presently studied mats, then younger, were previously studied quantitatively [10]. Here we employ, for the first time, a series of sections for the quantification of the biota of a complete microbial community. Other methods of

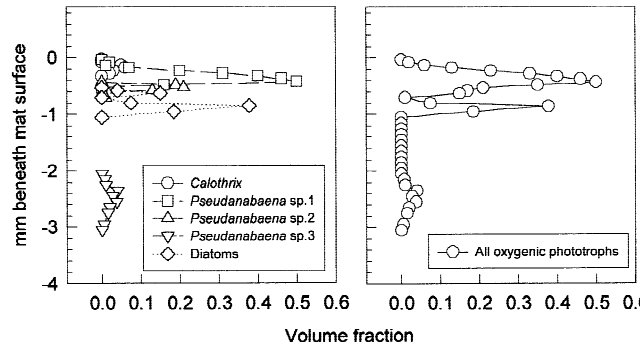

Fig. 7. Volume fraction of the dominant oxygenic phototrophs and of all oxygenic phototrophs as a function of depth.

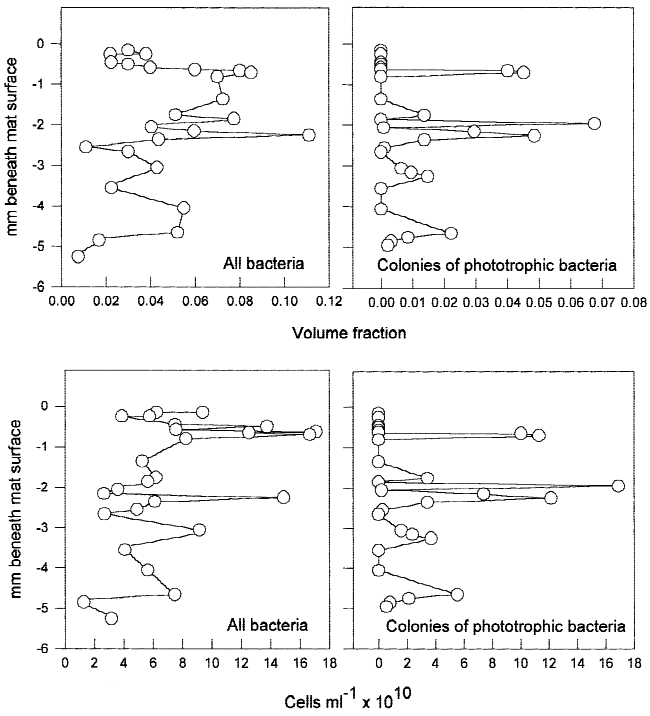

Fig. 8. Volume fraction and numbers of all bacteria and of colonial anoxygenic phototrophs as a function of depth.

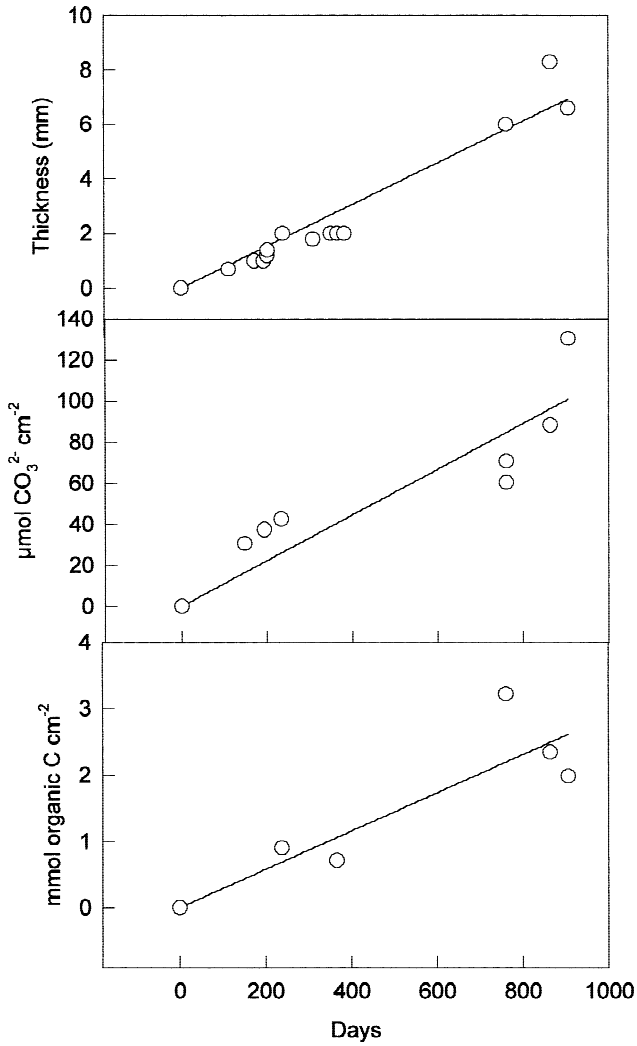

Fig. 9. Increment of mat thickness, carbonate and organic carbon content as a function of time.

visualization such as scanning electron microscopy and confocal microscopy [13, 19] do not provide means for quantification or for precise inference about three-dimensional relations inside intact, optically dense mats, or for the high resolution of detail that is possible by traditional (light and electron optical) microscopy on sectioned material. The application of freeze-sectioning for the study of the microdistribution of photosynthetic pigments is described in [14].

The studied mats have given an opportunity to study an undisturbed microbial community over a longer period of time. Comparisons with the mats when these were only a few months old [11] show that the basic structure and important constituents of the biota had in most respects not changed significantly. *Microcoleus chtonoplastes,* a cyanobacterium that dominates many other mats, had disappeared or become rare. On the other hand, *Phormidium* and *Calothrix* (incorrectly identified as *Nostoc* in [10]) had later become much more numerous. A number of eukaryotes (the diatom *Navicula,* the ciliate *Protocrucia,* an unidentified nematode, the rotifer *Colurella,* and unidentified amebae and heterotrophic flagellates) were common during the first year. Excepting the diatom and the small amebae, none were observed after 2.5 years and they must have become rare or extinct in the meantime.

In other respects the surface layers of the mats remained similar. This applies to the dominance of the three morphotypes of *Pseudanabaena* and their respective depth distributions and to the "plywood structure" of the cyanobacterial community in the upper 0.2 mm of the mat. The photosynthetic active zone of the mat therefore appears as a stable microbial community with few signs of successional changes. The mechanism behind the spatial ordering of cyanobacterial filaments remains unresolved: that is, whether photosensory motile behavior or, alternatively, geometric constraints in connection with filament reproduction is involved.

The basic vertical zonation patterns resembled that documented for natural cyanobacterial mats from saline lakes in most respects. The present mats are unusual in that diatoms

occurred beneath the bulk of the living cyanobacterial filaments rather than at the surface as recorded from most other mats (e.g., [5]).

The increment in mat thickness over time is also comparable to what has been found for natural stromatolitic mats, that is, between 0.5 and 5 mm per year (reviewed in [2]). Growth was primarily caused by the accumulation of empty cyanobacterial mucous sheaths and carbonate. The total amount of living biomass (wet weight) was estimated to be 0.055 g cm^{-2}. Assuming that the microbial biomass consists of 20% organic dry matter and that 50% of the organic dry matter is organic C, then this amounts to 0.46 mmol C cm^{-2} or roughly 20% of the organic C in the mat (cf Fig. 9). The remainder must be represented by the dead organic matrix. It has previously been shown for natural mats that cyanobacterial sheaths are surprisingly resilient to degradation [6, 8]. The carbonate deposits contribute less to the increment in mat thickness, but constitute (after 2.5 years) about 25% of the dry weight of the mat and probably contribute to its mechanical stability. They also affect the vertical light penetration in the mat [14].

It is generally assumed that the laminations characteristic of stromatolites and of recent stromatolitic mats reflect seasonal variation with respect to light and temperature or to sedimentation [8]. This could not apply to the presently studied mats. Nevertheless, they showed lamination in terms of discrete layers of carbonate. Their presence must somehow reflect the role of the mucous matrix in the layer of cyanobacterial filaments for carbonate precipitation [16] and suggests cycles of formation of an almost continuous carbonate layer followed by subsequent growth of cyanobacteria on its top.

Acknowledgments

We thank Birgit Brander, Ilse Duun, and Jeanne Sjřland Handest for technical assistance. Our studies were supported by grants from the Danish Natural Science Research Council to TF and MK.

References

1. Aherne WA, Dunnill MS (1982) Morphometry. Edward Arnold, London
2. Bauld J (1981) Occurrence of benthic microbial mats in saline lakes. Hydrobiologia 81:87–111
3. Microbial Mats: Stromatolites. Alan & Liss Inc, New York
4. Microbial Mats. Am Soc Microbiol, Washington, DC
5. D'Amelio ED, Cohen Y, Des Marais DJ (1989) Comparative functional ultrastructure of two hypersaline submerged cyanobacterial mats: Guerrero Negro, Baja California Sur, Mexico, and Solar Lake, Sinai, Egypt. In: Cohen Y, Rosenberg E (eds) Microbial Mats. Am Soc Microbiol, Washington, DC, pp 97–113
6. de Wit R, Grimelt JO, Hernadez-Mariné M (1994) Morphological and chemical transformations of *Microcoleus chthonoplastes* during early diagenesis in hypersaline microbial mats. In: Stal LJ, Caumette P (eds) Microbial Mats. Springer-Verlag, Berlin, pp 69–76
7. Elias H, Hennig A, Schwarz E (1971) Stereology: application to biomedical research. Physiol Rev 51:158–200
8. Farmer JD, Des Marais DJ (1994) Biological versus inorganic processes in stromatolite morphogenesis: observations from mineralizing sedimentary systems. In: Stal LJ, Caumette P (eds) Microbial Mats. Springer-Verlag, Berlin, pp 61–68
9. Fenchel T (1998) Formation of laminated cyanobacterial mats in the absence of benthic fauna. Aquat Microb Ecol 14:235–240
10. Fenchel T (1998) Artificial cyanobacterial mats: structure and composition of the biota. Aquat Microb Ecol 14:241–251
11. Fenchel T (1998) Artificial cyanobacterial mats: cycling of C, O and S. Aquat Microb Ecol 14:253–259
12. Javor BJ, Castenholz RW (1981) Laminated microbial mats, Laguna Guerrero Negro, Mexico. Geomicrobiol J 2:237–273
13. Jørgensen BB, Revsbech NP, Cohen Y (1983) Photosynthesis and structure of benthic microbial mats: microelectrode and SEM studies of four cyanobacterial communities. Limnol Oceanogr 28:1075–1093
14. Kühl M, Fenchel T (in press) Bio-optical characteristics and vertical distribution of photosynthetic pigments and photosynthesis in an artificial cyanbacterial mat. Microb Ecol
15. Nicholson JAM, Stolz JF, Pierson BK (1987) Structure of a microbial mat at Great Sippiwissett Marsh, Cape Cod, Massachussetts. FEMS Microbiol Ecol 45:343–364
16. Pentecost A, Bauld J (1988) Nucleation of calcite on the sheaths of cyanobacteria using a simple diffusion cell. Geomicrobiol J 6:129–135
17. Stolz JF (1983) Fine structure of the stratified microbial community at Laguna Figueroa, Baja California, Mexico. I. Methods of *in situ* study of laminated sediments. Precamb Res 20:479–492
18. Stolz JF (1994) Light and electron microscopy in microbial mat research: an overview. In: Stal LJ, Caumette (eds) Microbial Mats. Springer-Verlag, Berlin, pp 173–182
19. Wiggli M, Smallcombe A, Backhofen R (1999) Reflectance spectroscopy and laser confocal microscopy as tools in the ecophysiological study of microbial mats in an alpine bog pond. J Microbiol Methods 34:173–182